Journal of Alloys and Compounds, *177* (1991) 149–158
JAL 0049

Investigations on electronically conducting oxide systems XX. $MgNiMnO_4$ and properties of $Mg_zNiMn_{2-z}O_4$ spinels

A. Feltz and B. Neidnicht
Institute of Inorganic and Analytical Chemistry, Friedrich Schiller University, Jena (F.R.G.)

(Received June 8, 1991)

Abstract

Substitution of magnesium(II) for manganese in the series $Mg_z^{II}Ni^{II}Mn_z^{IV}Mn_{2-2z}^{III}O_4$ ($0 \leqslant z \leqslant 1$) yields spinels whose stability is increased in comparison with $NiMn_2O_4$ ($z=0$). Below 730 °C in air the latter compound is decomposed by oxidation, forming α-Mn_2O_3 and $NiMnO_3$. $MgNiMnO_4$ ($z=1$) is found to be stable on annealing at 450 °C. The change in electrical conductivity in the series from $\sigma_{20\,°C}=5\times10^{-4}\ \Omega^{-1}\ cm^{-1}$ ($E_\sigma=0.325$ eV) for $NiMn_2O_4$ ($z=0$) to $\sigma_{20\,°C}=5\times10^{-7}\ \Omega^{-1}\ cm^{-1}$ ($E_\sigma=0.392$ eV) for $MgNiMnO_4$ ($z=1$) is discussed.

1. Introduction

According to the phase diagram [1], $NiMn_2O_4$ used for thermistor applications [2–5] appears at room temperature in air as a metastable frozen-in state. This is certainly a disadvantage because the electrical properties tend to shift with time when the temperature is increasing [6]. The unstable nature of $NiMn_2O_4$ arises from the preference of nickel(II) to occupy octahedral sites. Therefore the cation distribution shows a comparatively high degree of inversion ($y \approx 0.65$–0.9 [7, 8]). Moreover, at least in part, p disproportionation of manganese(III) on the A sites of the spinel lattice has to be taken into account ($p \approx y$ [8, 9]):

$$Ni_{1-y}^{II}Mn_{y-p}^{III}Mn_p^{II}[Ni_y^{II}Mn_p^{IV}Mn_{2-y-p}^{III}]O_4 \qquad (1)$$

Since Mn_3O_4 is transformed into α-Mn_2O_3 below 935 °C in air [10], $NiMn_2O_4$ below 730 °C becomes oxidized to $Ni^{II}Mn^{IV}O_3$, whose structure (ilmenite type) obeys octahedral nickel(II) coordination, and at the same time α-Mn_2O_3 is formed.

In this paper appropriate cation substitution is proposed as a most promising route to form a stable spinel phase containing manganese(III) and manganese(IV) on the B sites as a prerequisite for sufficient electrical conductivity. Following the formula

$$Mg_z^{II}Ni_{1-z}^{II}[Ni_z^{II}Mn_z^{IV}Mn_{2-2z}^{III}]O_4 \quad \text{or}$$

$$Mg_z^{II}Ni_{1-y-z}^{II}Mn_{y-p}^{III}Mn_p^{II}[Ni_{y+z}^{II}Mn_{p+z}^{IV}Mn_{2-y-p-2z}^{III}]O_4 \qquad (2)$$

0925-8388/91/$3.50

substitution of magnesium(II) for manganese(III) implies the formation of manganese(IV) and at the same time nickel(II) should have the opportunity to change to the preferred octahedral B sites, because magnesium(II) is more suitable for A site occupation than nickel(II). As yet the spinel $MgNiMnO_4$ has not been found to be reported in the literature.

2. Preparation and X-ray diffraction measurements

Preparation has been tried according to formula (2) from mixtures of MgO and nickel and manganese carbonates with $z = \frac{1}{3}, \frac{2}{3}, \frac{5}{6}$ and 1. The powders were heated on 600 °C (3 h) for calcination, yielding a mixture consisting predominantly of MgO, NiO and α-Mn_2O_3 in the molar ratio under consideration. After densification by pressure sintering was carried out at 100 °C (20 h) in an oxygen atmosphere and after grinding, the procedure was repeated

TABLE 1

X-ray diffraction data for $MgNiMnO_4$ ($a_0 = 833.2 \pm 0.8$ pm)

d_{exp}	hkl	d_{ber}	$(I/I_0)_{exp}$	$(I/I_0)_{calc}$
4.822	111	4.809	80	49.9
2.940	220	2.945	16	8.5
2.512	311	2.512	100	100.0
2.404	222	2.405	23	11.2
2.085	400	2.083	68	60.4
1.910	331	1.911	4	11.7
1.701	422	1.700	4	3.3
1.603	511/333	1.603	25	32.5
1.473	440	1.473	45	57.7
1.408	531	1.408	7	8.6
	442	1.388	0	0.0
	620	1.317	0	1.3
1.270	533	1.270	9	10.2
1.257	622	1.256	7	7.8
1.202	444	1.202	7	9.3
	511/711	1.166	0	4.4
	642	1.113	0	1.4
1.084	553/731	1.085	10	17.9
1.041	800	1.041	5	8.3
	733	1.018	0	1.4
	644	1.010	0	0.0
	660/822	0.9817	0	0.8
0.9615	751/555	0.9619	6	11.4
	662	0.9555	0	4.5
0.9330	840	0.9313	8	15.6
	753/911	0.9143	0	4.4
	842	0.9083	0	0.0
	664	0.8880	0	0.5
0.8730	931	0.8732	8	10.5
0.8510	844	0.8502	10	33.0

twice more. For final treatment the powder samples have been annealed at 600 °C (40 h). At the different stages the composition of the powders was proved by dissolution of a weighing-out loss in diluted hydrochloric acid containing a definite concentration of iron(II) and titration with 0.1M Ce^{IV} solution. The procedure allows the determination of the average oxidation number of manganese. According to the formula

$$Mg_z^{II}Ni^{II}Mn_{2-z}^{II+k}O_{3+\delta} \qquad \text{with } k = \frac{2(2-z)+2\delta}{2-z} - 2 \tag{3}$$

$\delta = 1.00$ would refer to the formation of a homogeneous spinel phase.

However, the compounds could not be prepared in this way. Before NiO is involved in the formation process of the homogeneous spinel phase, ZnO becomes bound to Mn_2O_3, yielding spinels in the series $Zn_xMn_{3-x}O_4$ [11]. The reaction proceeds at sufficient rate at 800–900 °C [12, 13]. Already at about 700 °C $MgNiMnO_4$ ($z = 1$) becomes unstable. The value $\delta = 0.50$ experimentally observed after quenching from 1000 °C indicates a mixture of $\frac{1}{2}Mg_{1-a}Ni_aMn_2^{III}O_4$ and $\frac{3}{2}Mg_{1/3+a/3}Ni_{2/3-a/3}O$. Annealing at 600 °C yields $\delta = 0.79$. Starting from the oxide mixture, the formation of the homogeneous spinel phase becomes extremely extended in time at the lower temperature.

Preparation of the spinels succeeds following the oxalate route [1, 14–17]. The decomposition of mixed crystals of $Mg_zNiMn_{2-z}(C_2O_4)_3 \cdot 6H_2O$ prepared from aqueous solution was found to be complete at 440 °C in an oxygen atmosphere. Thermal decomposition of $NiMn(C_2O_4)_2 \cdot 4H_2O$ leads already at 330 °C to the formation of cubic defect spinels [18]. In the system under consideration oxygen contamination is observed in the range 460–650 °C, yielding cubic spinels of definite composition ($\delta = 1.00$).

The X-ray diffraction data of $MgNiMnO_4$ are summarized in Table 1, indicating sufficient agreement with the values calculated with the LAZY PULVERIX programme [19]. $MgNiMnO_4$ forms a cubic spinel lattice with $a_0 = 833.2$ pm. Obviously, nickel(II) and manganese(IV) are randomly distributed on the B sites. No indications of ordering have been observed in the X-ray diffraction diagram.

As shown in Fig. 1, indicated deviations from Vegard's rule are in the series of substitution. The lattice parameters are collected in Table 2 together with the onset of thermal decomposition at the upper (HT) and lower (LT) temperatures.

3. Thermal decomposition of the compounds

$NiMn_2O_4$ ($z = 0$) becomes decomposed in the HT range above 975 °C in an oxygen atmosphere [20]:

$$NiMn_2O_4 \xrightarrow[O_2]{>975\ ^\circ C} xNiO + \frac{3-x}{3} Ni_{(3-3x)/(3-x)}^{II}Mn_{2x/(3-x)}^{II}Mn_2^{III}O_4 + \frac{x}{6} O_2 \tag{4}$$

Obviously, because of the formation of manganese(IV), the onset temperature of oxygen liberation is decreasing in the series $Mg_z^{II}Ni^{II}Mn_z^{IV}Mn_{2-2z}^{III}O_4$ ($0 \leqslant z \leqslant 1$).

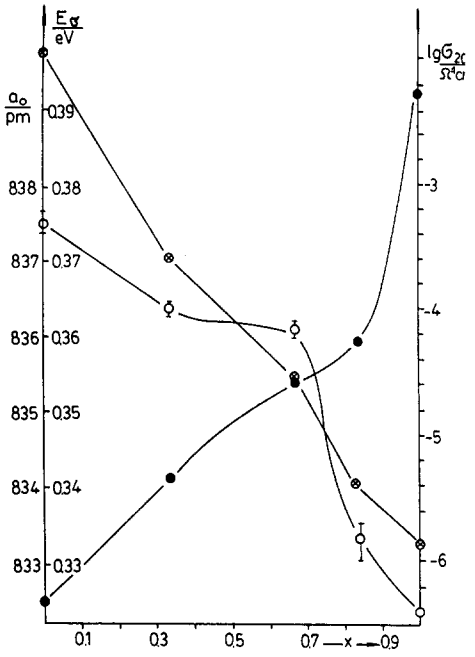

Fig. 1. Lattice parameter a_0 (⊗) and variation in activation energy E_σ (●) and electrical conductivity $\sigma_{20\,°C}$ (○) as a function of compositional parameter x in the series $Mg_xNiMn^{III}_{2-2x}Mn^{IV}_xO_4$.

TABLE 2

Lattice parameters and values of thermal decomposition of the spinels $Mg_zNiMn_{2-z}O_4$ ($0 \leqslant z \leqslant 1$)

Compound	a_0 (pm)	$\rho_{X\text{-ray}}$ (g cm^{-3})	T_{dec}(HT) (O_2 atmosphere) (°C)	T_{dec}(LT) (air) (°C)
$NiMn_2O_4$	839.7 ± 0.2	5.339	> 975	< 730
$Mg_{1/3}NiMn_{5/3}O_4$	837.0	5.037	> 860	< 650
$Mg_{2/3}NiMn_{4/3}O_4$	835.4	4.834	> 820	< 450
$Mg_{5/6}NiMn_{7/6}O_4$	834.0	4.742	> 730	< 450
$MgNiMnO_4$	833.2 ± 0.8	4.638	> 720	Stable

Figure 2 shows the curve of thermal decomposition of $MgNiMnO_4$ ($z = 1$) up to 1200 °C measured with a heating rate of 10 K min^{-1}. Starting from the powder state of decomposed $MgNiMnO_4$, re-oxidation takes place completely if a cooling rate of 1 K min^{-1} is applied. On the other hand, compact ceramic samples ($\rho_{rel} = 70\%$) need a longer annealing time, about 70 h at 650 °C, for re-oxidation.

X-ray diffraction measurements and the analytical determination of the degree of oxidation applied to samples quenched from 1200 °C allow the assumption of a mixture of an NiO-rich NaCl-type phase and a tetragonal

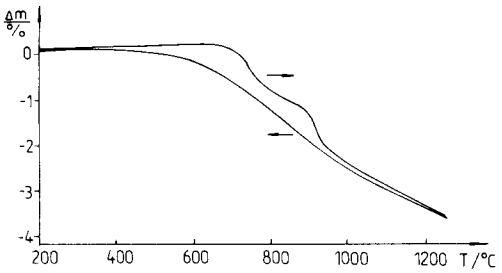

Fig. 2. Thermogravimetric measurement of decomposition of $MgNiMnO_4$ in oxygen; heating rate 10 K min^{-1}, cooling rate 1 K min^{-1}.

spinel whose composition is close to $MgMn_2O_4$ ($\delta = 0.50$). $\delta = 0.51$ is found. $\delta = 0.72$ and the pattern of a cubic spinel is observed after quenching from 1000 °C, suggesting a mixture which could be approximated by NiO and $\frac{2}{3}Mg^{II}(Mg^{II}_{1/2}Mn^{IV}_{1/2}Mn^{III})O_4$ in accordance with the phase diagram of the system $Mg_xMn_{3-x}O_4$ [21]. Obviously, in contrast to the more separated mixtures discussed in the previous section, the intimate mixture of the two phases formed by decomposition of the spinels gives rise to successful re-formation of the spinel on annealing at lower temperature.

In the LT range below about 730 °C $NiMn_2O_4$ is also unstable, but now because of oxidation yielding $NiMnO_3$ and α-Mn_2O_3:

$$NiMn_2O_4 + \tfrac{1}{4}O_2 \longrightarrow NiMnO_3 + \tfrac{1}{2}\alpha - Mn_2O_3 \qquad (5)$$

Indeed, the data of Table 2 give experimental evidence for an effect of stabilization if magnesium is substituted for manganese in the series. $Mg_{1/3}NiMn_{5/3}O_4$ ($z = \frac{1}{3}$) is formed at 800 °C. As for $NiMn_2O_4$, decomposition takes place; however, the temperature of the onset of instability appears to be decreased from 720 to 650 °C. The spinel $Mg_{2/3}NiMn_{4/3}O_4$ ($z = \frac{2}{3}$) was found to remain unchanged at 650 °C for 100 h. However, at 450 °C for 1200 h decomposition also proceeds. A value of $\delta = 1.11$ is found, although X-ray diffraction shows only the pattern of a single cubic spinel phase. An analogous result has been obtained for $Mg_{5/6}NiMn_{7/6}O_4$ ($z = \frac{5}{6}$). The compound seems to be stable at 650 °C. Nevertheless, thermal stability also fails. $\delta = 1.04$ was found after 600 h annealing at 450 °C.

On the other hand, $MgNiMnO_4$ ($z = 1$) was proved to be a stable compound. During annealing at 450 °C (720 h) the state of $MgNiMnO_4$ remained completely unchanged ($\delta = 1.00$).

4. Electrical conductivity and magnetic measurements

Conductivity measurements require compact samples of definite geometry prepared by sintering at higher temperatures. In order to obtain tablets of sufficient density, small discs (diameter 5 mm, height 2 mm) have been formed by application of pressure utilizing a powder with a specific surface area $S = 4$ m^2 g^{-1}. Granulometric pretreatment adding 5% of an aqueous

solution of 5% PVA allowed the achievement of a green density of 52% of the theoretical value. Moreover, for sintering support by liquid phase formation 1 mol.% of the spinel has been substituted by $(Pb_5Ge_3O_{12})_{3/8}$. Sintering was carried out at 1000 °C (2 h) in an oxygen atmosphere followed by annealing at 650 °C (50 h) for re-oxidation. The latter needs a residual porosity of the samples.

The d.c. conductivity of the samples with fired silver contacts was measured between 20 and 70 °C using the voltage drop method equipped with a constant-current source [22, 23]. The data summarized in Table 3 have been plotted together with the lattice parameters in Fig. 1. Although the molar volume is shrinking by about 1.6% between $NiMn_2O_4$ ($x=0$) and $MgNiMnO_4$ ($x=1$), the activation energy of the electrical conductivity is increasing by about 20%. Subsequently, the room temperature conductivity is decreasing by about three orders of magnitude.

The magnetic properties of the compounds paramagnetic at room temperature yielding μ_{exp} are in sufficient agreement with the values μ_{eff} calculated utilizing the magnetic moments for manganese(II) (5.7–6.1 μ_B), manganese(III) (4.8–4.9 μ_B), manganese(IV) (3.8–4.0 μ_B) and nickel(II) (2.8–3.5 μ_B) [24]. The data collected in Table 4 have been obtained by measuring the magnetic susceptibility with the Gouy method. Neither the degree of inversion y nor

TABLE 3

Analytical data and electrical conductivity of sintered and re-oxidized samples of the series $Mg_zNiMn_{2-z}O_{3+\delta}$

Compound	ρ_{rel} (%)	δ	$\sigma_{20\,°C}$ (Ω^{-1} cm^{-1})	B (K)	E_σ (eV)
$NiMn_2O_{4.00}$	96	1.00	$(5\pm1)\times10^{-4}$	3774 ± 3	0.325
$Mg_{1/3}NiMn_{5/3}O_{4.04}$	81	1.04	$(1.1\pm0.2)\times10^{-4}$	3956 ± 7	0.341
$Mg_{2/3}NiMn_{4/3}O_{4.00}$	94	1.00	$(6.7\pm0.3)\times10^{-5}$	4100 ± 5	0.353
$Mg_{5/6}NiMn_{7/6}O_{4.00}$	80	1.00	1.4×10^{-6}	4166 ± 35	0.358
$MgNiMnO_{4.00}$	70	1.00	4×10^{-7}	4550	0.392

TABLE 4

Magnetic properties of spinel compounds in the series $Mg_zNi^{II}_{1-y-z}Mn^{III}_{y-p}Mn^{II}_p[Ni^{II}_{y+z}Mn^{IV}_{p+z}Mn^{III}_{2-y-p-2z}]O_4$

Compound	$10^4\,\chi_{m(20\,°C)}$ (cm^3 mol^{-1})	T_N (K)	θ_p (K)	C (K cm^3 mol^{-1})	μ_{exp} (μ_B)	μ_{calc} (μ_B)
$NiMn_2O_{4.00}$	116.1	88	−280	6.86	7.41	7.43–8.02
$Mg_{1/3}NiMn_{5/3}O_{4.04}$	93.9	80	−315	5.77	6.73	6.62–7.28
$Mg_{2/3}NiMn_{4/3}O_{4.00}$	88.4	80	−231	4.61	6.07	5.79–6.04
$Mg_{5/6}NiMn_{7/6}O_{4.00}$	—	—	—	—	—	—
$MgNiMnO_4$	63.1	82	−201	3.276	5.12	4.72–5.32

the share p of disproportionation is resolved at this stage of analysis of the magnetic data.

5. Discussion of the results

For a detailed discussion, comparison of the molar volumes in the series of manganese-containing spinels MMn_2O_4 is suggested to be helpful. The data collected in Fig. 3 reveal a distinct difference between the tetragonally distorted spinels Mn_3O_4, $FeMn_2O_4$, $CoMn_2O_4$, $ZnMn_2O_4$ and $MgMn_2O_4$, characterized by a higher molar volume and lower electrical conductivity, and those of higher density packing such as $NiMn_2O_4$ and $CuMn_2O_4$, whose conductivity is increased coupled with a lowering of the activation energy. The Jahn–Teller effect causes distortion of the compounds in the former group. Mn_3O_4, $ZnMn_2O_4$ and $MgMn_2O_4$ show normal cation site occupation and the conductivity is lower the higher the molar volume. $FeMn_2O_4$, obtainable only on quenching at reduced oxygen partial pressure, has been proposed to be in a cation distribution state of $Fe^{III}_{1/3}Mn^{II}_{2/3}[Mn^{III}Mn^{II}_{1/3}Fe^{III}_{2/3}]O_4$ [25]. The higher conductivity of $CoMn_2O_4$ has been traced back to a small share of inversion with disproportionation of manganese(III) according to formula (1) [26].

On the other hand, $NiMn_2O_4$, driven to inversion by the octahedral site preference of nickel(II), certainly contains a higher share of manganese(IV). The formula

$$Ni^{II}_{1/3}Mn^{III}_{2/3-p}Mn^{II}_{p}[Ni^{II}_{2/3}Mn^{III}_{4/3-p}Mn^{IV}_{p}]O_4 \qquad (6)$$

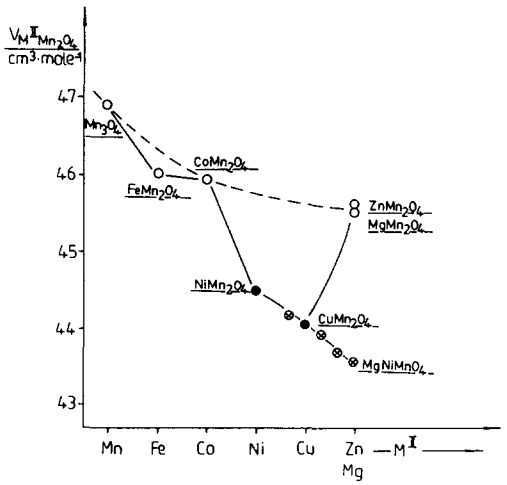

Fig. 3. Molar volume and electrical properties of manganite spinels MMn_2O_4: (○) Mn_3O_4 – $E_\sigma = 1.67$ eV [34], $E_\sigma = 1.3$, 1.0 eV, $\sigma_{20\,°C} = 10^{-12}\ \Omega^{-1}\ cm^{-1}$ [35]; $FeMn_2O_4$ [25]; $CoMn_2O_4$ – $E_\sigma = 0.394$ eV, $\sigma_{20\,°C} = 4.0 \times 10^{-6}\ \Omega^{-1}\ cm^{-1}$ [26], $E_\sigma = 0.405$ eV, $\sigma_{20\,°C} = 8.4 \times 10^{-5}\ \Omega^{-1}\ cm^{-1}$ [36]; $ZnMn_2O_4$ – $E_\sigma = 0.85$ eV, $\sigma_{20\,°C} = 2.1 \times 10^{-7}\ \Omega^{-1}\ cm^{-1}$ [37]; $MgMn_2O_4$ – $E_\sigma = 1.05$ eV, $\sigma_{20\,°C} = 7.9 \times 10^{-8}\ \Omega^{-1}\ cm^{-1}$ [37]; (●) $NiMn_2O_4$ – $E_\sigma = 0.246$ eV, $\sigma_{20\,°C} = 5.0 \times 10^{-4}\ \Omega^{-1}\ cm^{-1}$; $CuMn_2O_4$ – $E_\sigma = 0.20$ eV, $\sigma_{20\,°C} = 0.14\ \Omega^{-1}\ cm^{-1}$ [26, 38]; (⊗) $Mg_zNiMn_{2-z}O_4$ ($0 \leqslant z \leqslant 1$).

with $y=\frac{2}{3}$ and p close to y has been shown to be the best approximation to experimental results [8, 9, 18]. Macroscopically, the diminished part of manganese(III) allows suppression of Jahn–Teller distortion because of the prevailing influence of nickel(II) and manganese(IV) maintaining undistorted octahedral symmetry on the B sites. Manganese(IV) gives rise to increased covalent bond interaction and closer particle packing, which appears as the source for providing the energy required for disproportionation. At the same time, increased $Mn^{IV}-O$ bond interaction is expected to lower the temperature of oxygen release. Indeed, in comparison with the tetragonally distorted spinels of the former group the onset of thermal decomposition of $NiMn_2O_4$ is decreased by several hundred degrees to about 950 °C in air. Following formula (2) and starting from $NiMn_2O_4$ ($z=0$), the manganese(IV) content is increasing with z and subsequently the molar volume is further decreasing in the series studied, which is shown in Fig. 3. Subsequently, at the same time the temperature of decomposition (HT) is lowered to 720 °C (Table 2).

Taking into account the manganese(IV) formation as the main reason for molar volume shrinkage, the positive deviation from Vegard's rule shown in Figs. 1 and 2 suggests partial lowering of the disproportionation parameter p (formula (2)) in the series of substitution. The degree of inversion y, obeying the condition $y<1-z$, also becomes reduced step by step in the series.

The electrical charge carrier transport has to be described by hopping between the B sites of the spinel lattice occupied by manganese(III) and manganese(IV). Considering the activation energy, substantial potential fluctuations have to be taken into account. Therefore, as for studies carried out in the spinel series $Mg^{II}[Mg_x^{II}Ti_x^{IV}Ti_{2-2x}]O_4$ [27, 28], the polaron-hopping energy must be considerably increased by the barriers resulting from disorder of randomly distributed cations when the charge difference is growing in the series of substitution. The thermopower of $NiMn_2O_4$ was found to show only a low temperature dependence, which is in accordance with the conclusions deduced from thermopower measurements of $Mg^{II}[Mg_{0.5}^{II}Ti_{0.5}^{IV}Ti^{III}]O_4$ ($x=0.5$) [27].

Presumably, in the range $0\leqslant z\leqslant\frac{2}{3}$ the increase in activation energy and lowering of the conductivity as shown in Fig. 2 have to be traced back to further growth of potential fluctuations. Starting from formula (6) ($z=0$, $y=\frac{2}{3}$, p close to y) and assuming the maintenance of $y=\frac{2}{3}$, the formula

$$Mg_{1/3}Mn_{2/3-p}^{III}Mn_p^{II}[Ni^{II}Mn_{1/3+p}^{IV}Mn_{2/3-p}^{III}]O_4 \qquad \text{at } z=\tfrac{1}{3} \tag{7}$$

appears to be plausible. At the next step the degree of inversion has to be reduced to $y=\frac{1}{3}$, yielding

$$Mg_{2/3}Mn_{1/3-p}^{III}Mn_p^{II}[Ni^{II}Mn_{2/3+p}^{IV}Mn_{1/3-p}^{III}]O_4 \qquad \text{at } z=\tfrac{2}{3} \tag{8}$$

In the whole range $0<z<\frac{2}{3}$ the value $p<y$ seems to be smaller than $p\approx y$ as assumed for $z=0$, which is in accordance with the conductivity data as well as with the positive deviation of the molar volume. In the range

$\frac{2}{3} < z < 1$ the value of p approximates more and more to $y < 1 - z$, leading to the low conductivity of $Mg(Ni^{II}Mn^{IV})O_4$.

For completion, $CuMn_2O_4$ showing a molar volume comparable with that of $NiMn_2O_4$ has also been picked up in Fig. 3. Tetrahedral copper(I) in the presence of octahedral manganese(IV) has been proposed from structural and magnetic measurements [25, 29–31]. The cation distribution $Cu^{II}_{0.48}Cu^{I}_{0.28}Mn^{II}_{0.24}[Cu^{II}_{0.24}Mn^{III}_{1.24}Mn^{IV}_{0.52}]O_4$ was deduced from X-ray photoelectron spectroscopy measurements [32, 33]. The degree of inversion is lower than for $NiMn_2O_4$. On the other hand, manganese(IV) formation seems to be supported by copper(I) formation. Obviously, the share of copper(II) and manganese(III) cations on the octahedral B sites is high enough to induce tetragonal distortion ($a_0 = 825$ pm, $c_0 = 863$ pm). The low electrical resistivity is proposed to be caused by a polaron-hopping mechanism Cu^{I}–$Mn^{IV} \rightleftharpoons Cu^{II}$–$Mn^{III}$ involving an interaction between A and B site cations in addition to the Mn^{III}–Mn^{IV}-hopping events within the B site sublattice.

Acknowledgments

We thank Dr. Schirrmeister for measuring the conductivity data and Dipl.-Chem. Schütze for carrying out the magnetic measurements.

References

1 D. Wickham, *J. Inorg. Nucl. Chem.*, *26* (1964) 1369.
2 B. Boucher, R. Buhl and M. Perrin, *C. R. Acad. Sci.*, *263* (1966) 344.
3 H. Walch, *Siemens-Zeitschr.*, *47* (1973) 66.
4 S. Sakkar, M. L. Sharma, H. L. Bhaskar and K. C. Nagpal, *J. Mater. Sci.*, *19* (1984) 545.
5 T. Yamamoto, Y. Yoshida, H. Igarashi and K. Okazaki, *Adv. Ceram.*, *15* (1986) 237.
6 A. Feltz, J. Töpfer and F. Schirrmeister, *J. Eur. Ceram. Soc.*, in the press.
7 M. S. Islam and C. R. A. Catlow, *J. Phys. Chem. Solids*, *49* (1988) 119.
8 E. G. Larson and R. J. Arnott, *J. Phys. Chem. Solids*, *23* (1962) 1771.
9 E. D. Macklen, *J. Phys. Chem. Solids*, *47* (1986) 1073.
10 A. Feltz, W. Ludwig and Ch. Felbel, *Z. Anorg. Allg. Chem.*, *540–541* (1986) 36.
11 F. C. M. Driessens and G. D. Rieck, *J. Inorg. Nucl. Chem.*, *28* (1966) 1593.
12 A. Feltz and M. Jäger, *React. Solids*, *6* (1988) 119.
13 A. Feltz and M. Jäger, *Hermsdorfer Techn. Mitt.*, *78* (1990) 2494.
14 D. Dollimore and D. Nicholson, *J. Chem. Soc.*, (1962) 960.
15 D. Dollimore and D. L. Griffiths, *J. Chem. Soc.*, (1963) 2617.
16 V. A. M. Brabers and J. C. J. M. Terhell, *Phys. Status Solidi A*, *69* (1982) 325.
17 E. Jarby, R. A. Boissier, R. Carnet and A. Lagrange, *J. Phys. (Paris), Colloq. CI, Suppl. 2*, *47* (1986) 843.
18 A. Feltz and J. Töpfer, *Z. Anorg. Allg. Chem.*, *576* (1989) 71.
19 K. Yvon, W. Jeitschko and E. Parthe, *J. Appl. Crystallogr.*, *10* (1977) 73.
20 J. Jung, J. Töpfer, J. Mürbe and A. Feltz, *J. Eur. Ceram. Soc.*, *6* (1990) 351.
21 B. P. Barchatow and J. W. Golikow, *Dokl. Akad. Nauk SSSR*, *252* (1980) 383.
22 F. Schirrmeister and A. Feltz, *Phys. Status Solidi A*, *57* (1980) 591.
23 F. Schirrmeister and A. Blayer, *Hermsdorfer Techn. Mitt.*, *30* (1990) 2481.
24 A. Weiss and H. Witte, *Magnetochemie*, Grundlagen und Anwendungen Verlag Chemie, Weinheim, 1972.

25 A. P. B. Sinha, N. R. Sinjana and A. B. Biswas, *Acta Crystallogr., 10* (1957) 439.
26 S. T. Kshirsagar and C. D. Sabane, *Jpn. J. Appl. Phys., 10* (1971) 794.
27 A. Feltz and M. Steinbrück, *J. Less-Common. Met., 167* (1991) 233.
28 A. Feltz, M. Steinbrück, P. Dordor and J. P. Doumerc, *Eur. J. Solid State Inorg. Chem.*, in the press.
29 G. Blasse, *J. Phys. Chem. Solids, 27* (1966) 383.
30 R. Buhl, *J. Phys. Chem. Solids, 30* (1969) 805.
31 R. E. Vandenberg, G. G. Robbrecht and V. A. M. Brabers, *Phys. Status Solidi A, 34* (1976) 583.
32 M. J. Dreiling, *J. Phys. Chem. Solids, 37* (1976) 121.
33 M. Lenglet, A. D'Huysser, J. Kasperek, J. P. Bonnelle and J. Durr, *Mater. Res. Bull., 20* (1985) 745.
34 S. E. Dorris and T. O. Mason, *J. Am. Ceram. Soc., 71* (1988) 379.
35 B. Gillot, M. Kharroubi, R. Metz, R. Legros and A. Rousset, *Phys. Status Solidi A, 124* (1991) 317.
36 A. Feltz and M. Ottlinger, *Z. Chem., 29* (1969) 338.
37 M. Rosenberg, P. Nicolau, R. Manaila and P. Pausescu, *J. Phys. Chem. Solids, 24* (1963) 1419.
38 S. T. Kshirsagar, *J. Phys. Soc. Jpn., 27* (1969) 1164.